

Reliable and efficient operation of distribution network by connecting solar distributed generation

Simarla Vijender Reddy, Mane Manjula

Department of Electrical Engineering, University College of Engineering, Osmania University, Hyderabad, India

Article Info

Article history:

Received Oct 27, 2022

Revised Jan 9, 2023

Accepted Jan 25, 2023

Keywords:

Distributed generation

Distribution network

MOSMA

Power loss

Solar energy

Voltage regulation

ABSTRACT

One of the major issues in the distribution network (DN) is ensuring that power systems operate optimally in light of the effects of distributed generation (DG). In a broader sense, optimal operation in a power system refers to the most efficient use of all active and reactive power generation and control equipment that adheres to physical and technical constraints. Most studies focused on DG size and location in the DN, using various optimization techniques for loss reduction. But in a practical distribution network, reliable operation is dependent on the demand and power supply at any given moment. Solar DGs provide variable power throughout the day, and loads are similarly variable. It is difficult for the DN to function efficiently and reliably while handling variable loads and DG power supplies. Voltages and power losses are measured as loads change by connecting solar DGs to assess the performance of the DN.

This is an open access article under the [CC BY-SA](#) license.



Corresponding Author:

Simarla Vijender Reddy

Department of Electrical Engineering, University College of Engineering, Osmania University

Hyderabad, Telangana 500007, India

Email: simarlavijender@gmail.com

1. INTRODUCTION

Electrical power demand is increasing day by day to meet the escalating electrical power usage. The majority of electricity sources currently are conventional. The availability of conventional energy sources is dwindling by the day. Non-conventional energy sources, such as wind and solar, are plentiful. Renewable energy sources are the best option for meeting power demand. The optimal allocation problems are solved using optimization techniques such as the genetic algorithm (GA), particle swarm optimization (PSO), ant colony search algorithm (ACSA), slime mould algorithm (SMA), and multi-objective slime mould algorithm (MOSMA).

Almabsout *et al.* [1] addresses controlling active and reactive power in distribution networks has a significant impact on their performance. The most common strategies for improving distribution system performance are the connection of distributed generation (DG) and shunt capacitors (SCs). The reactive power optimization algorithm for distribution network (DN) with solar (PV) generation is provided in [2]. The penetration of renewable distributed generation (RDG) into traditional distribution systems (TDSs) is examined in [3] and has been found to address many of its flaws and shortcomings. According to [4], installing local micro-level power generating sources such as fuel cells, micro turbines, and energy storage devices is a current trend that aids in the intermittent impacts of renewable energy sources while making micro grids less reliant on the main grid.

According to [5], the significant level of penetration of such renewable energy sources has an effect on the dynamic performance of power systems. The regulations for wind power plants are to protect the boundaries that maintain the reliable operation of the power system. The stochastic optimal power flow

(OPF) problem is addressed in [6] by a robust and effective method inspired by the slime mould. As per [7], [8], the installation of a DG at a grid node minimizes real power losses in the network. The slime mould optimization approach is used to manage the reactive power (Volt/VAr) of smart inverters for PVs in order to optimize PVHC in DN [9]. Premkumar *et al.* [10] covers the use of MOSMA in the industry to solve multi-objective optimization problems. Ouyang *et al.* [11] proposed the theory and method of active and reactive power coordinated control before wind speed changes on the basis of model predictive control theory. According to [12], it is a slow occurrence that can be handled utilizing slow manual reserves. If these reserves must be obtained from nearby regions, they should be kept at a sufficient reserve capacity in the AC tie-lines. According to [13], the frequency regulation strategy that merely responds to traditional power is progressively reduced as wind power becomes more integrated into the electric system.

Singh *et al.* [14] presents a multimode single-stage solar photovoltaic (PV) energy generation system (SPEGS) interfaced to a distribution feeder using a reliable DS-based control technique that has been created for enhancing power quality. Kim and Lee [15] presents a two-stage probabilistic forecasting system for solar power that makes use of observations of solar irradiation taken at various sites. A two-stage robust optimal inverter dispatch model has been presented to manage the uncertainties of PV generation in active distribution networks [16], [17]. By combining solar and wind turbines in addition to the current grid, it is possible to provide consumers with an uninterrupted power supply at a low cost [18]. Ghiassi-Farrokhfal *et al.* [19] examined the challenge of allocating a capital budget to solar panels stored in the context of a large-scale solar farm engaging in an energy market in order to optimize predicted revenue.

Chang *et al.* [20] presents an improved backward/forward sweep methodology for the three-phase load-flow analysis of radial distribution systems. A strategy for solving the distributed power flow problem that is adaptive and relies on compensation. This approach was examined under a variety of scenarios, including load imbalance, an abrupt increase in 1-phase loads, the degree of meshing in the loops, and the number of generating nodes. It is quick, reliable, and keeps the required accuracy [21], [22]. A linear three-phase power flow model for a DN is covered in [23], [24].

2. RENEWABLE ENERGY SOURCES

There are numerous renewable energy sources available, including solar, wind, biomass, geothermal, biodiesel, biogas, tidal energy, and others. Solar energy is the best choice for large-scale power generation. Solar power applications are used in this paper. Solar panels produce changeable power as the temperature varies throughout the day, from sunrise to sunset. Solar panels generate maximum power at a temperature of 25 °C. The solar power generation is nil during the nighttime.

3. LOAD FLOW ANALYSIS

Load flow is used to evaluate voltages at each node and power losses at each branch of the distribution network. The effective power of each node is evaluated using the bus injected node power (BINP) matrix. The effective line resistance of each node is determined using the line loss node power (LLNP) matrix [25], [26]. The equivalent two-node DN is shown in Figure 1.

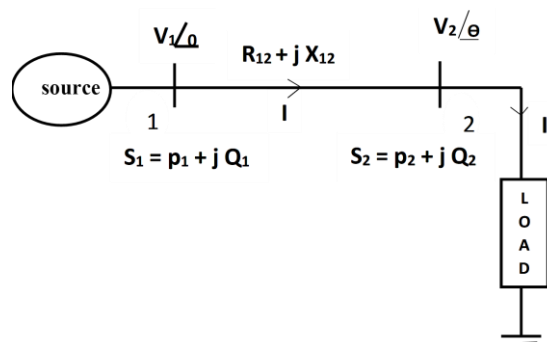


Figure 1. 2-bus distribution network

The voltage at any node for sending end 'M' and receiving end 'N' is given by (1).

$$V_N = V_{N-1} - \left(\frac{P_{Neff} \times R_{M,N} + Q_{Neff} \times X_{M,N}}{V_{N-1}} \right) + j \left(\frac{Q_{Neff} \times R_{M,N} - P_{Neff} \times X_{M,N}}{V_{N-1}} \right) \quad (1)$$

Where P_{Neff} and Q_{Neff} are active and reactive powers at 'N' nodes respectively. The power loss of 'N' buses DN is shown in (2).

$$P_{loss} = \sum_{k=2}^N I_k^2 \times R_{k-1,k}$$

Where 'k' represents the kth node of DN and $I_k^2 = \left(\frac{S_k}{V_k}\right)^2$.

$$P_{loss} = \sum_{k=2}^N \left(\frac{S_k}{V_k}\right)^2 \times R_{k-1,k} \quad (2)$$

The IEEE 85-bus radial DN is shown in Figure 2. The line impedances and node powers are given in [26]. The total load power of DN is 3640 kVA at a power factor of 0.8 lag.

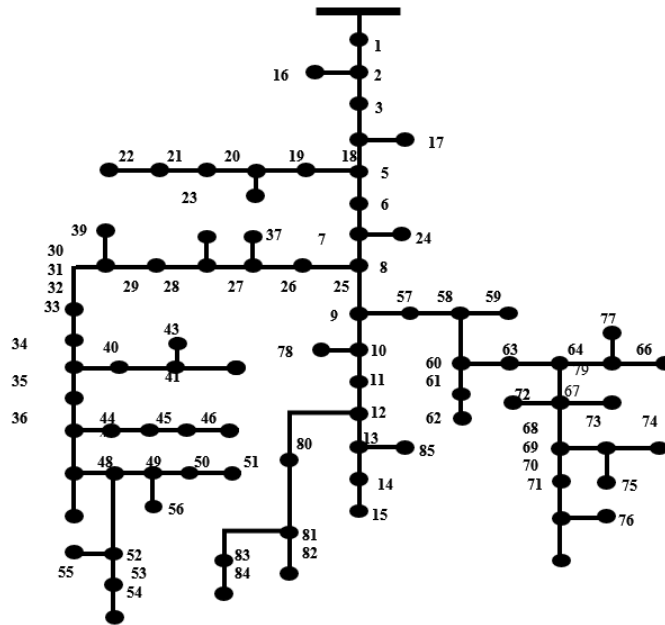


Figure 2. 85-Bus radial distribution network

4. SLIME MOULD AND MULTI-OBJECTIVE SLIME MOULD ALGORITHM

Slime mould algorithm (SMA), predicted the existence of a novel inhabitant of a location-based metaheuristic seemingly moved by supernatural powers by the swinging manner of conduct of slime mould fashionable nature. The input positions of slime mould are declared as $X=(X_1, X_2, X_3, \dots, X_N)$. Where 'N' is the population size, the population is judged by utilizing an objective function. The staging process of the SMA algorithms, which involves grasping edible material, wrapping food, and approaching edible material, can be specified mathematically as (3).

$$\begin{cases} X = ra.(U - L) + L, & \text{if}(ra < .03) \\ X = X_A(t) + VA.(W.X_a(t) - X_b(t)), & \text{if}(rand < q) \\ X = vC.X(t), & \text{if}(rand \geq q) \end{cases} \quad (3)$$

"W" represents the smell index, "VA" is the vibration limit, and the lower and upper limits of the search area are represented by "L" and "U". The 'rand' and "ra" are represented as random values. The slime mould has been represented as a DG location and size in this slime mould algorithm.

MOSMA is a variant of SMA that incorporates non-dominated sorting and crowding distance [6]. In this paper, the multi-objective slime mould method is used to focus on power loss minimization and reduce voltage deviation, whereas the slime mould algorithm is used to focus on single objectives such as power loss minimization. Power loss reduction and voltage deviation are calculated using (4) and (5), respectively.

$$P_{loss} = \sum_{k=2}^n \left(\frac{S_k - S_{GK}}{V_k}\right)^2 \times R_{k-1,k} \quad (4)$$

$$V_{mag} = \sum_{i=2}^N |V_{REF} - V_i| \quad (5)$$

Algorithm for MOSMA

- i) Read initial parameters (Ua, La, N, Max.Iter=100).
- ii) Read the Line and load data.
- iii) Initially, generate the slime mould (DG location and size).
- iv) Run load flow (calculate voltages and power losses from (1) and (2)).
- v) Modify the slime mould from (3).
- vi) Non-dominated sorting from (4) and (5) (power loss and voltage deviation for different slime moulds).
- vii) Crowding distance between power loss and voltage deviation for different slime moulds.
- viii) Check to converge? (No to go to step iii), Yes to print results).

5. RESULTS AND DISCUSSION

The performance of the IEEE-85 bus radial DN is determined by calculating voltages and power losses.

5.1. IEEE-85 bus radial distribution network results

The 85 buses of voltages are depicted in Figure 3. On 85 buses, the lowest voltage available is 0.877 per unit (PU), which is less than the 0.95 PU boundary limit. The DN has a power loss of 320.7 kVA. In this state, the DN has been unreliable and inefficient. The performance of DN is evaluated by linking solar DGs.

5.1.1. Solar results

Solar DGs are placed and sized optimally in 85 bus DN using various optimization techniques such as SMA and MOSMA. Table 1 shows the placements and sizes of solar DGs for various optimization techniques. The MOSMA method has higher per-unit voltages for 85 buses than the SMA, as shown in Figure 4. The power losses of SMA and MOSMA are 95.1 kVA and 97.6 kVA, respectively.

The irradiance of the sun varies throughout the day, from dawn to sunset. The output power of solar panels varies with temperature. As the power supplied by solar DGs varies, the voltages of DN fluctuate. The DN supplies are reliable if the voltages on all buses are within the limits. The voltages for several case studies of solar DGs with variable power supply are assessed.

Solar DGs produce their maximum power when the sun is shining at a temperature of 25 °C. Solar DGs produce the least amount of power at sunrise, then climb to their maximum, and finally decline to their minimum at dusk. Solar DGs generate power at 50%, 75%, and 100% of their maximum capacity, as shown in Table 2. The minimum voltages at 75% and 50% of maximum power solar DGs, as shown in Figure 5, are 0.944 and 0.922 per unit, respectively, which are outside of the boundary limits.

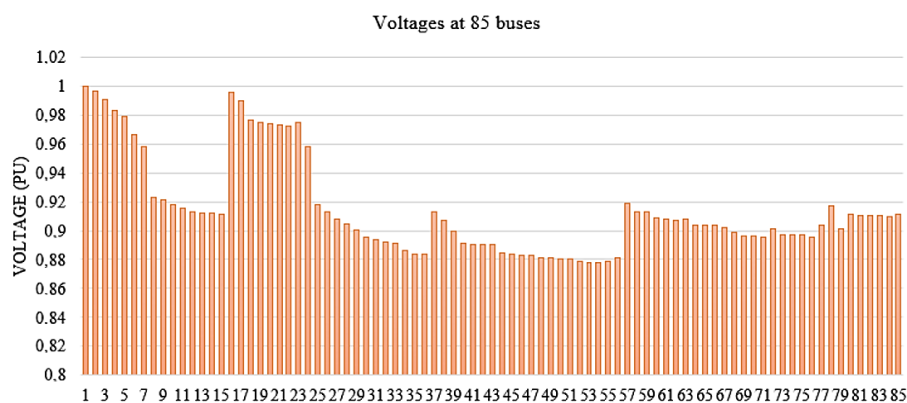


Figure 3. Voltages at 85 buses

Table 1. Solar DGs placement and power supply in 85 bus DN

Solar DG Number	MOSMA		SMA	
	Place at Bus no.	Power supply (kVA)	Place at Bus no.	Power supply (kVA)
DG_1	34	432.6	55	430.0
DG_2	74	413.5	31	421.1
DG_3	51	477.5	10	404.2
DG_4	82	384.6	80	452.9
DG_5	62	457.1	70	459.0

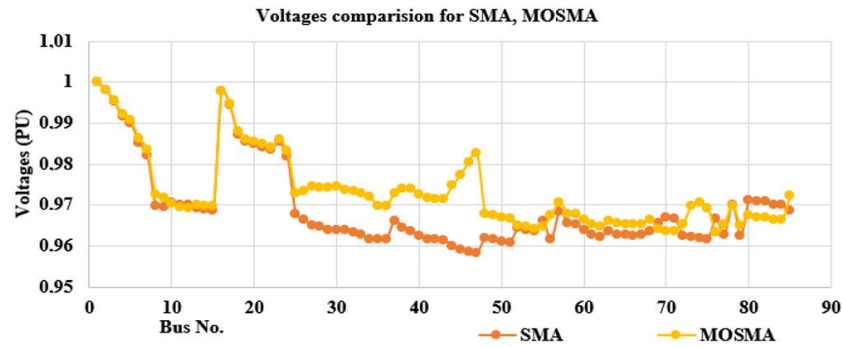


Figure 4. Voltages at 85 buses for SMA and MOSMA

Table 2. The various power supply of solar DGs

Solar DGs place	Solar DGs at the maximum power supply		One of 5 DGs at 50% of maximum power supply		Two of 5 DGs at 50% of the maximum power supply		5 DGs at 75% of maximum power supply		5 DGs at 50% of maximum power supply	
	DGs number	Power supply (kVA)	Change at DGs	power supply (kVA)	Change at DGs	power supply (kVA)	Change at DGs	power supply (kVA)	Change at DGs	power supply (kVA)
34	DG_1	432.6	DG_1	432.6	DG_1	432.6	75% of DG_1	324.4	50% of DG_1	216.3
74	DG_2	413.5	DG_2	413.5	DG_2	413.5	75% of DG_2	310.1	50% of DG_2	206.7
51	DG_3	477.5	DG_3	477.5	DG_3	477.5	75% of DG_3	358.1	50% of DG_3	238.7
82	DG_4	384.6	DG_4	384.6	50% of DG_4	192.3	75% of DG_4	288.5	50% of DG_4	192.3
62	DG_5	457.1	50% of DG_5	228.5	50% of DG_5	228.5	75% of DG_5	342.8	50% of DG_5	228.5

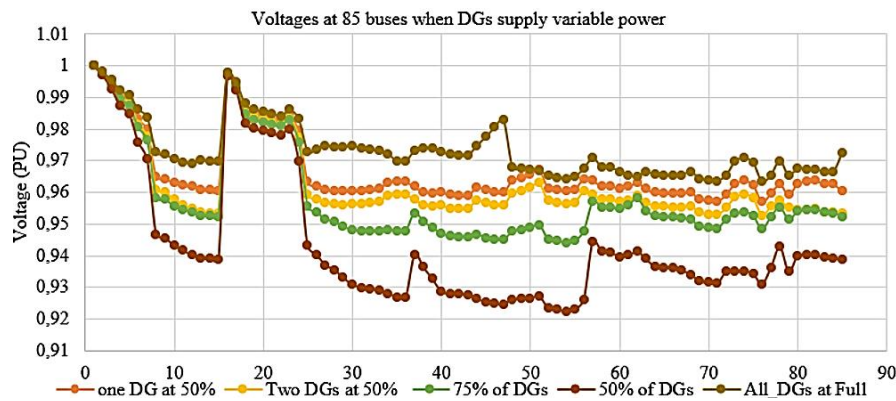


Figure 5. Voltages at 85 buses with variable power supply of solar DGs

The output power of solar DGs diminishes dramatically under cloudy conditions. Cloudy conditions in one or two locations cause a significant drop in solar DG power, which has an effect on DN voltages. Due to cloudy conditions, the DG 4 and DG 5 powers have been reduced by 50% and are connected to 82 and 62 buses, respectively, as shown in Table 2. The corresponding voltages of 85 buses are shown in Figure 5. Even though the power of two DGs has been reduced by 50% owing to cloudy weather, the voltages are within the boundary limitations. The power losses of DN with variable power sources of solar DGs are depicted in Figure 6.

The voltages in the distribution network change as the supply power or the load varies. The voltages of 85 buses are evaluated with load changes when solar DGs generate maximum power, as shown in Table 2. Figure 7 shows the voltages of 85 buses with load variations of 50%, 75%, 100%, and 125%, all of which are within the boundary limits except for the load change of 125%. The lowest voltage at 125% load is 0.932 per unit, making the power supply for the loads unreliable. Figure 8 shows the power losses with varying loads, with the lowest losses occurring at 50% load.

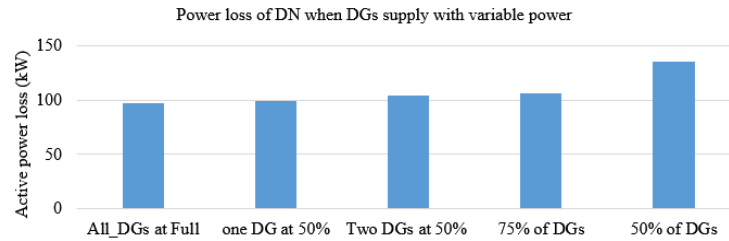


Figure 6. power losses at 85 buses with variable power supply of solar DGs

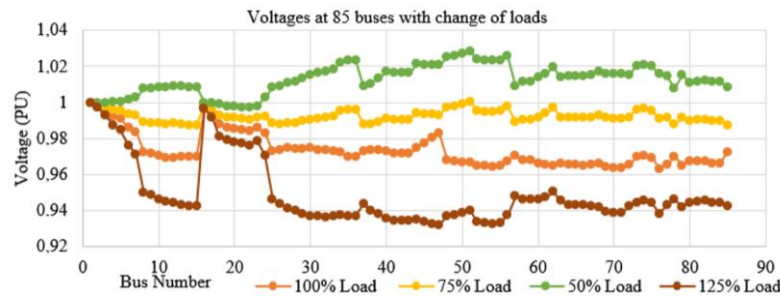


Figure 7. Voltages at 85 buses with variable loads

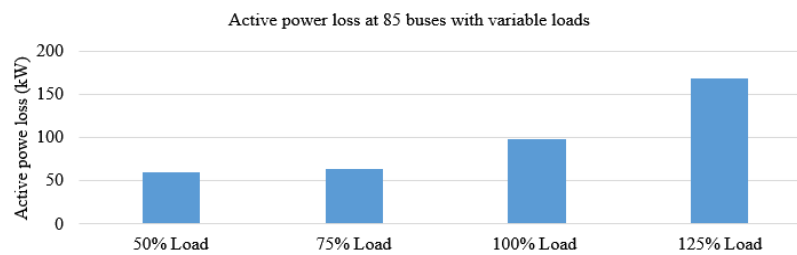


Figure 8. Power losses at 85 buses with variable loads

6. CONCLUSION

Solar DGs are placed and sized optimally in 85 buses DN using SMA and MOSMA. The MOSMA approach performed better than others in terms of the two objectives, which are voltage improvement and power loss reduction, than others. The DN has been reliable even when the power of one or two solar DGs has been reduced to 50% of maximum power, but the DN has been unreliable when the power of all solar DGs has dropped to 75% of maximum power. When solar DGs are connected, voltages decrease as the load increases. At 125% of full load, power losses are larger and voltages are felt below the boundary limits, making the distribution network unreliable.





REFERENCES

- [1] E. A. Almabsout, R. A. El-Sehiemy, O. N. U. An, and O. Bayat, "A hybrid local search-genetic algorithm for simultaneous placement of DG units and shunt capacitors in radial distribution systems," *IEEE Access*, vol. 8, pp. 54465–54481, 2020, doi: 10.1109/ACCESS.2020.2981406.
- [2] Y. Ai, M. Du, Z. Pan, and G. Li, "The optimization of reactive power for distribution network with PV generation based on NSGA-III," *CPSS Transactions on Power Electronics and Applications*, vol. 6, no. 3, pp. 193–200, Sep. 2021, doi: 10.24295/cpsstpea.2021.00017.
- [3] H. M. H. Farh, A. M. Al-Shaalan, A. M. Eltamaly, and A. A. Al-Shamma'A, "A novel crow search algorithm auto-drive PSO for optimal allocation and sizing of renewable distributed generation," *IEEE Access*, vol. 8, pp. 27807–27820, 2020, doi: 10.1109/ACCESS.2020.2968462.
- [4] M. Yousif, Q. Ai, Y. Gao, W. A. Wattoo, Z. Jiang, and R. Hao, "An optimal dispatch strategy for distributed microgrids using PSO," *CSEE Journal of Power and Energy Systems*, vol. 6, no. 3, pp. 724–734, Jun. 2020, doi: 10.17775/CSEEJPES.2018.01070.
- [5] O. M. Kamel, A. A. Z. Diab, T. D. Do, and M. A. Mossa, "A novel hybrid ant colony-particle swarm optimization techniques based tuning STATCOM for grid code compliance," *IEEE Access*, vol. 8, pp. 41566–41587, 2020, doi: 10.1109/ACCESS.2020.2976828.
- [6] S. Mouassa, A. Althobaiti, F. Jurado, and S. S. M. Ghoneim, "Novel design of slim mould optimizer for the solution of optimal power flow problems incorporating intermittent sources: a case study of Algerian electricity grid," *IEEE Access*, vol. 10, pp. 22646–22661, 2022, doi: 10.1109/ACCESS.2022.3152557.





- [7] F. F. Amigue, S. N. Essiane, S. P. Ngoffe, G. A. Ondo, G. M. Mengounou, and P. T. Nna Nna, "Optimal integration of photovoltaic power into the electricity network using slime mould algorithms: application to the interconnected grid in North Cameroon," *Energy Reports*, vol. 7, pp. 6292–6307, Nov. 2021, doi: 10.1016/j.egy.2021.09.077.
- [8] G. Kou *et al.*, "Load rejection overvoltage of utility-scale distributed solar generation," *IEEE Transactions on Power Delivery*, vol. 35, no. 4, pp. 2113–2116, Aug. 2020, doi: 10.1109/TPWRD.2019.2951949.
- [9] R. A. Ibrahim, D. Yousri, M. Abd Elaziz, S. Alshathri, and I. Attiya, "Fractional calculus-based slime mould algorithm for feature selection using rough set," *IEEE Access*, vol. 9, pp. 131625–131636, 2021, doi: 10.1109/ACCESS.2021.3111121.
- [10] M. Premkumar, P. Jangir, R. Sowmya, H. H. Alhelou, A. A. Heidari, and H. Chen, "MOSMA: multi-objective slime mould algorithm based on elitist non-dominated sorting," *IEEE Access*, vol. 9, pp. 3229–3248, 2021, doi: 10.1109/ACCESS.2020.3047936.
- [11] J. Ouyang, M. Li, Z. Zhang, and T. Tang, "Multi-timescale active and reactive power-coordinated control of large-scale wind integrated power system for severe wind speed fluctuation," *IEEE Access*, vol. 7, pp. 51201–51210, 2019, doi: 10.1109/ACCESS.2019.2911587.
- [12] K. Das, F. Guo, E. Nuño, and N. A. Cutululis, "Frequency stability of power system with large share of wind power under storm conditions," *Journal of Modern Power Systems and Clean Energy*, vol. 8, no. 2, pp. 219–228, 2020, doi: 10.35833/MPCE.2018.000433.
- [13] P. Yang *et al.*, "Research on primary frequency regulation control strategy of wind-thermal power coordination," *IEEE Access*, vol. 7, pp. 144766–144776, 2019, doi: 10.1109/ACCESS.2019.2946192.
- [14] A. K. Singh, S. Kumar, and B. Singh, "Solar PV energy generation system interfaced to three phase grid with improved power quality," *IEEE Transactions on Industrial Electronics*, vol. 67, no. 5, pp. 3798–3808, May 2020, doi: 10.1109/TIE.2019.2921278.
- [15] H. Kim and D. Lee, "Probabilistic solar power forecasting based on bivariate conditional solar irradiation distributions," *IEEE Transactions on Sustainable Energy*, vol. 12, no. 4, pp. 2031–2041, Oct. 2021, doi: 10.1109/TSTE.2021.3077001.
- [16] H. Shaker, H. Zareipour, and D. Wood, "Estimating power generation of invisible solar sites using publicly available data," *IEEE Transactions on Smart Grid*, vol. 7, no. 5, pp. 2456–2465, Sep. 2016, doi: 10.1109/TSG.2016.2533164.
- [17] T. Ding, C. Li, Y. Yang, J. Jiang, Z. Bie, and F. Blaabjerg, "A two-stage robust optimization for centralized-optimal dispatch of photovoltaic inverters in active distribution networks," *IEEE Transactions on Sustainable Energy*, vol. 8, no. 2, pp. 744–754, Apr. 2017, doi: 10.1109/TSTE.2016.2605926.
- [18] B. Priyadharshini, V. Ganapathy, and P. Sudhakara, "An optimal model to meet the hourly peak demands of a specific region with solar, wind, and grid supplies," *IEEE Access*, vol. 8, pp. 13179–13194, 2020, doi: 10.1109/ACCESS.2020.2966021.
- [19] Y. Ghiassi-Farokhfal, F. Kazhamiaka, C. Rosenber, and S. Keshav, "Optimal design of solar PV farms with storage," *IEEE Transactions on Sustainable Energy*, vol. 6, no. 4, pp. 1586–1593, Oct. 2015, doi: 10.1109/TSTE.2015.2456752.
- [20] G. W. Chang, S. Y. Chu, and H. L. Wang, "An improved backward/forward sweep load flow algorithm for radial distribution systems," *IEEE Transactions on Power Systems*, vol. 22, no. 2, pp. 882–884, May 2007, doi: 10.1109/TPWRS.2007.894848.
- [21] S. Wang, Q. Liu, and X. Ji, "A fast sensitivity method for determining line loss and node voltages in active distribution network," *IEEE Transactions on Power Systems*, vol. 33, no. 1, pp. 1148–1150, Jan. 2018, doi: 10.1109/TPWRS.2017.2735898.
- [22] M. Bazrafshan and N. Gatsis, "Convergence of the Z-bus method for three-phase distribution load-flow with ZIP loads," *IEEE Transactions on Power Systems*, vol. 33, no. 1, pp. 153–165, Jan. 2018, doi: 10.1109/TPWRS.2017.2703835.
- [23] Y. Wang, N. Zhang, H. Li, J. Yang, and C. Kang, "Linear three-phase power flow for unbalanced active distribution networks with PV nodes," *CSEE Journal of Power and Energy Systems*, vol. 3, no. 3, pp. 321–324, Oct. 2017, doi: 10.17775/CSEEJPES.2017.00240.
- [24] J. A. D. Massignan, B. R. Pereira, and J. B. A. London, "Load flow calculation with voltage regulators bidirectional mode and distributed generation," *IEEE Transactions on Power Systems*, vol. 32, no. 2, pp. 1576–1577, 2017, doi: 10.1109/TPWRS.2016.2576679.
- [25] J. B. V. Subrahmanyam and C. Radhakrishna, "A simple method for optimal capacitor placement in unbalanced radial distribution system," *Electric Power Components and Systems*, vol. 38, no. 11, pp. 1269–1284, Aug. 2010, doi: 10.1080/15325001003670910.
- [26] D. Das, D. P. Kothari, and A. Kalam, "Simple and efficient method for load flow solution of radial distribution networks," *International Journal of Electrical Power & Energy Systems*, vol. 17, no. 5, pp. 335–346, Oct. 1995, doi: 10.1016/0142-0615(95)00050-0.

BIOGRAPHIES OF AUTHORS



Simarla Vijender Reddy     was born in Charakonda village, Nagerkarnool district, Telangana State, India. He received M.Tech. degree from Jawaharlal Nehru Technology University Hyderabad (JNTUH). He is pursuing P.hD. at Osmania University. Currently, he is working as an Assistant Professor in the Department of Electrical Engineering, UCE, Osmania University. He has more than 12 years of experience in teaching. His research area is application of optimization techniques in power systems. He can be contacted at email: simarlavijender@gmail.com.



Mane Manjula     completed her B.E in Electrical and Electronics Engineering from Osmania University in the year 1995. She joined the Department of Electrical Engineering, University College of Engineering, Osmania University in 1997 as a lecturer. Completed her Ph.D. in the year January 2014. She is having 24 years of teaching experience in the field of Electrical Engineering. She is presently working as Professor in the Department. She can be contacted at email: vijendersimarla100@gmail.com.